New Phytologist

An aquaporin PvTIP4;1 from *Pteris vittata* may mediate arsenite uptake

Zhenyan He[1]*, Huili Yan[1,2]*, Yanshan Chen[1,2]*, Hongling Shen[1,2], Wenxiu Xu[1], Haiyan Zhang[1], Lei Shi[1], Yong-Guan Zhu[3] and Mi Ma[1]

[1]Key Laboratory of Plant Resources, Institute of Botany, Chinese Academy of Sciences, Beijing 100093, China; [2]University of Chinese Academy of Sciences, Beijing 100049, China; [3]Key Laboratory of Urban Environment and Health, Institute of Urban Environment, Chinese Academy of Sciences, Xiamen 361021, China

Authors for correspondence:
Mi Ma
Tel: +0086 10 62836255
Email: mami@ibcas.ac.cn

Yong-Guan Zhu
Tel: +86 592 6190997
Email: ygzhu@iue.ac.cn

Received: *17 April 2015*
Accepted: *5 August 2015*

New Phytologist (2016) **209:** 746–761
doi: 10.1111/nph.13637

Key words: aromatic/arginine (Ar/R), arsenic (As), arsenite (As(III)), aquaporin, *Pteris vittata*, *PvTIP4;1*, uptake.

Summary

- The fern *Pteris vittata* is an arsenic hyperaccumulator. The genes involved in arsenite (As (III)) transport are not yet clear. Here, we describe the isolation and characterization of a new *P. vittata* aquaporin gene, *PvTIP4;1*, which may mediate As(III) uptake.
- *PvTIP4;1* was identified from yeast functional complement cDNA library of *P. vittata*. Arsenic toxicity and accumulating activities of *PvTIP4;1* were analyzed in *Saccharomyces cerevisiae* and *Arabidopsis*. Subcellular localization of PvTIP4;1–GFP fusion protein in *P. vittata* protoplast and callus was conducted. The tissue expression of *PvTIP4;1* was investigated by quantitative real-time PCR. Site-directed mutagenesis of the PvTIP4;1 aromatic/arginine (Ar/R) domain was studied.
- Heterologous expression in yeast demonstrates that PvTIP4;1 was able to facilitate As(III) diffusion. Transgenic *Arabidopsis* showed that *PvTIP4;1* increases arsenic accumulation and induces arsenic sensitivity. Images and FM4-64 staining suggest that PvTIP4;1 localizes to the plasma membrane in *P. vittata* cells. A tissue location study shows that *PvTIP4;1* transcripts are mainly expressed in roots. Site-directed mutation in yeast further proved that the cysteine at the LE1 position of PvTIP4;1 Ar/R domain is a functional site.
- PvTIP4;1 is a new represented tonoplast intrinsic protein (TIP) aquaporin from *P. vittata* and the function and location results imply that *PvTIP4;1* may be involved in As(III) uptake.

Introduction

The wide distribution of toxic arsenic (As) in soil and water is of great concern with respect to adverse health effects (Hayes, 1997; Jarup, 2003; Mudhoo *et al.*, 2011; Yang, 2011). It occurs predominantly in an inorganic form as arsenate (As(V)) and arsenite (As(III)) (Cullen & Reimer, 1989).

The first known arsenic hyperaccumulation fern, *Pteris vittata* (brake fern), is highly efficient in a range of inorganic and organic arsenic species for extraction of this metal from the soil and for arsenic translocation into its fronds (Ma *et al.*, 2001; Wang *et al.*, 2011). Although As(III) is predominant under anaerobic conditions, it is also present in aerobic environments where As(V) typically dominates (Wang *et al.*, 2011), for example as a result of biochemical transformation by plant roots (Xu *et al.*, 2007) and microbially mediated As(V) reduction (Yamamura *et al.*, 2008). As(III) accounts for an important part of arsenic pools in plant rhizospheres and in aerobic soils.

The mechanisms of arsenic hyperaccumulation in *P. vittata* include the process of arsenic uptake, reduction, efflux and sequestration. In the last few years, molecular mechanisms of As hyperaccumulation in *P. vittata* have been widely studied. PvACR2 is a specific glutathione-dependent As(V) reductase and plays an important role in As(V) reduction in the roots of *P. vittata* (Duan *et al.*, 2005; Ellis *et al.*, 2006). Expressing *PvTPI* in bacterial cells can also show that the gene has a role in As(V) reduction (Rathinasabapathi *et al.*, 2006). PvGrx5, a plant glutaredoxin, was reported to have a role in arsenic tolerance and homeostasis via improving As(V) reduction and regulating cellular arsenic levels (Sundaram *et al.*, 2008). As(III) antiporter gene *PvACR3* was identified and found to be necessary for arsenic tolerance in *P. vittata* gametophytes, indicating that *PvACR3* likely effluxes As(III) into the vacuole for sequestration (Indriolo *et al.*, 2010). Expressing *PvACR3* in *Arabidopsis thaliana* further proved that *PvACR3* can mediate As(III) efflux (Chen *et al.*, 2013). The identification of these genes and proteins provides insight into the dissection of the molecular mechanisms of arsenic hyperaccumulation of this extraordinary fern. The genes required for arsenic tolerance and hyperaccumulation, for example, As(III) uptake, however, are still not clear yet in *P. vittata*.

The major intrinsic protein (MIP) family is a family of channel proteins and can be classified as aquaporins (AQPs; water channels) and aquaglyceroporins (GLPs; glycerol intrinsic proteins) (Heymann & Engel, 1999). In higher plants, the

*These authors contributed equally to this work

MIP family can be classified into seven plant-specific subgroups: plasma membrane intrinsic proteins (PIPs), tonoplast intrinsic proteins (TIPs), the nodulin-26 like intrinsic proteins (NIPs), the small basic intrinsic proteins (SIPs), hybrid intrinsic proteins (HIPs), the uncategorized X intrinsic proteins (XIPs) and the GlpF-like intrinsic proteins (GIPs) (Weig *et al.*, 1997; Chaumont *et al.*, 2001; Quigley *et al.*, 2002; Danielson & Johanson, 2008). Based on phylogenetic comparisons, PIPs, TIPs, NIPs, HIPs, XIPs and SIPs belong to the AQPs (Johanson *et al.*, 2001) and GIPs are regarded as GLPs (Gustavsson *et al.*, 2005). MIPs can function as channels facilitating the movement of water and/or small neutral solutes, which include As(III) in a wide variety of organisms.

To date, several MIPs have been reported to be involved in As (III) transport. The *Escherichia coli* aquaglyceroporin, GlpF (Meng *et al.*, 2004), and the *Saccharomyces cerevisiae* aquaglyceroporin, Fps1p (Wysocki *et al.*, 2001), are membrane proteins that have been demonstrated to transport As(III). It has been shown that mammalian aquaglyceroporins, AQP9 and AQP7, may be major routes of As(III) uptake into mammalian cells (Liu *et al.*, 2002). Recently, it was reported that OsNIP2;1 (Lsi1) of *Oryza sativa* was an As(III) channel responsible for arsenic accumulation in rice grains (Ma *et al.*, 2008). Moreover, *OsNIP1;1*, *OsNIP2;2* (Lsi6) and *OsNIP3;1* all showed their permeability to As(III) in *Xenopus laevis* oocytes (Ma *et al.*, 2008). The members of the rice PIP subfamily, *OsPIP2;4*, *OsPIP2;6* and *OsPIP2;7*, are also involved in As(III) transport (Mosa *et al.*, 2012). In *Arabidopsis*, *NIP1;1*, *NIP2;1*, *NIP3;1*, *NIP5;1* and *NIP7;1* are permeable to As(III) and the disruption of these genes decreases the As concentration in plants (Bienert *et al.*, 2008; Isayenkov & Maathuis, 2008; Kamiya *et al.*, 2009; Xu *et al.*, 2015). Other NIPs, such as *AtNIP6;1* and *AtNIP7;1* from *Arabidopsis* and *LjNIP5;1* and *LjNIP6;1* from *Lotus japonicas*, are also permeable to As(III) (Bienert *et al.*, 2008).

TIP is a subfamily of AQPs that was first called TP25 for it is a tonoplast protein (Johnson *et al.*, 1989, 1990). Based on sequence homology, TIPs have been further classified into six distinct groups, which include TIP1, TIP2, TIP3, TIP4, TIP5 (Chaumont *et al.*, 2001; Quigley *et al.*, 2002) and TIP6, specifically expressed in *Physcomitrella patens* (Danielson & Johanson, 2008). Some TIPs have been detected to be predominantly located at the tonoplast (Johnson *et al.*, 1989; Hofte *et al.*, 1992; Daniels *et al.*, 1996). However, the subcellular distribution of TIPs might be more complex than previously thought (Barkla *et al.*, 1999). Fluorescence signals of AtTIP2;1 and AtTIP1;2 are localized not merely to the tonoplast, but in several endosomal membrane compartments. In addition, AtTIP4;1-derived fluorescence was hardly detectable in the tonoplast, whereas the signal in released material including plasma membrane remained stronger (Liu *et al.*, 2003). Phylogenetic and signal peptide analyses and *GFP* fusion experiments confirmed that AtTIP5;1 is an aquaporin with mitochondrial localization (Soto *et al.*, 2010). Studies have shown that AtTIP4;1 can mediate the transport of water to regulate water flow in response to drought and salinity stress. In addition to its role as a water channel proteins, AtTIP4;1 also transports urea (Liu *et al.*, 2003).

The structures of AQPs have been solved at atomic resolution by X-ray crystallography. AQPs comprise six membrane-spanning α-helices and five loops located on the intra- or extracytoplasmic side of the membrane (Fu *et al.*, 2000). The N-terminal extremity of AQP displays *c.* 20% conservation with the C-terminal extremity (Wistow *et al.*, 1991). It has been reported that C- and N-terminal domains of AQP are important for the transport activity (Cabello-Hurtado & Ramos, 2004). N-terminal truncation of AtNIP5;1, AtNIP6;1 (Bienert *et al.*, 2008) and C-terminal truncation of AtNIP3;1 have significant effect on As(III) transport capacity (Xu *et al.*, 2015).

Sequence analysis reveals the presence of a highly conserved aromatic/arginine (Ar/R) signature sequence motif in AQPs (Agre & Kozono, 2003). The Ar/R region consists of a spatial arrangement of residues from helices 2 (H2), helices 5 (H5), and loop E (LE1 and LE2) (Stroud *et al.*, 2003). The current view holds that the Ar/R region acts as a size-exclusion barrier and serves as a selectivity filter for the transport of substrates (Sui *et al.*, 2001). For instance, the substitution of the amino acid at the H5 position of OsLsi1 results in a total loss of Si and boron transport activities and a partial loss of As(III) transport activity (Mitani-Ueno *et al.*, 2011).

In the present work, to select genes that mediate As(III) uptake in *P. vittata*, the yeast As(III) uptake mutant *Δfps1* (Wysocki *et al.*, 2001) was transformed with a cDNA library from *P. vittata*. We identified a new TIP4-like aquaporin protein in *P. vittata* with an As(III) sensitive transformant. We employed As (III) transport activity assays of the aquaporin protein in yeast mutants and transgenic plants as well as subcellular and tissue localization studies.

Materials and Methods

Isolation of *PvTIP4;1*

A full-length cDNA library was constructed from RNA purified from *Pteris vittata* L. grown in As(III)-free and As(III)-containing medium, using Gateway technology (CloneMiner cDNA Library Construction Kit; Invitrogen). Then the full-length cDNA sequences were transferred into the yeast expression vector *pAG413GAL-ccdB* containing a His selectable marker by an attL and attR recombination reaction (LR reaction). The library was transformed into the As(III)-resistant yeast strain *Δfps1* and transformants were directly plated onto As(III)-selective medium (SD-His with 1 mM As(III), 2% galactose/glucose, and 2% (w/v) agarose). As(III) sensitive transformants were selected and the cDNA sequences were isolated and sequenced.

Protein structure and phylogenetic analysis

The PvTIP4;1 sequence was analyzed using DNAMAN and displayed using TMRPres2D (Spyropoulos *et al.*, 2004) to determine the position of the transmembrane helices. The amino acid sequences of PvTIP4;1, ScFps1 and AQPs from *Physcomitrella patens*, *Arabidopsis thaliana* and *Oryza sativa* were aligned and a phylogenetic tree was constructed using neighbour-joining

distance methods (Poisson model) in MEGA version 5.05 (Tamura *et al.*, 2011). Bootstraps were performed with 10 000 replications. The amino acid sequences of PvTIP4;1 and TIP4s in plants were aligned using DNAMAN (Lynnon Biosoft, Quebec, Canada) software according to the default program configuration. The obtained comparisons were saved as *.seq files in GCG format (accepted by the GENEDOC program). Edition of alignments using GENEDOC tools was conducted. The GenBank accession numbers of all sequences are listed in Supporting Information Table S1.

Yeast arsenic toxicity and transport activities assays

The constructed vectors *PvTIP4;1-pAG413GAL* along with the empty vector *pAG413GAL* using the CloneEZ PCR Cloning Kit (Genscript Co., Nanjing, China), were transformed into *Saccharomyces cerevisiae Δfps1* and *Δacr3* mutant. The methods related to yeast cultures, transformations and growth assays mainly referred to the book 'Methods in yeast genetics: a Cold Spring Harbor laboratory course manual' (Adams *et al.*, 1997). Yeast cells were grown at 30°C in synthetic defined (SD) medium (0.67% yeast nitrogen base, Sigma) without amino acids, containing 2% (w/v) glucose or 2% (w/v) galactose (induction medium), supplemented with yeast synthetic dropout without histidine (Clontech, CA, USA), pH 5.8.

For the arsenic toxicity assay, yeast was diluted by sterile water to an OD_{600} of 1.0, 0.1, 0.01 and 0.001. The drop assays were performed on SD-His plates (with 2% (w/v) galactose/glucose) containing 0 and 1.0 mM sodium As(III) for the yeast transformants of *Δfps1* or 0 and 0.2 mM As(V) for the yeast transformants of *Δacr3*.

For arsenic toxicity growth curve assay, yeast was diluted by 20 ml liquid SD-His + gal medium to an OD_{600} of 0.1 in 100 ml triangular flasks containing 100 μM sodium As(III) for the yeast transformants of *Δfps1* and 200 μM sodium As(V) for the yeast transformants of *Δacr3*. Then the triangular flasks were incubated at 30°C ar 200 rpm and the OD_{600} values of the medium were measured after 0, 6, 12, 18 or 24 h.

For the arsenic accumulation test, the yeast transformants of *Δfps1* were grown in liquid SD medium (with 2% (w/v) galactose) to an OD_{600} of 1.0 containing 100 μM sodium As(III) for 0.5, 1 or 2 h or in 20, 50 or 100 μM sodium As(III) for 0.5 h. The yeast transformants of *Δacr3* were grown in liquid SD medium (with 2% (w/v) galactose) to an OD_{600} of 1.0 containing 100 μM sodium As(V) for 4, 8 or 12 h or in 20, 50 or 100 μM sodium As(V) for 4 h. The yeast samples were collected after centrifuging and washing for three times with distilled water.

All the assays were performed at least three times.

Arabidopsis arsenic toxicity and accumulation assays

PvTIP4;1 was cloning into the CaMV 35S promoter cassette of *pSN1301* and transformed into *Arabidopsis thaliana* Col-0 by an *Agrobacterium*-mediated dip flora transformation (Clough & Bent, 1998). Transgenic plants in the T_2 generation were selected using primers with the following sequences: *PvTIP4;1* Fw: ATGCCTCTCCGCAACATTGCCCTCG; *PvTIP4;1* Rv: TCAGTAGTCCTGATCAGCAGAGGAG. The *pSN1301* vector was used as control. All the plants were grown at 22°C under a 16 h:8 h, light:dark photoperiod.

For seed germination observation, 50 seeds were incubated for 2 d at 4°C and placed horizontally on half-strength Murashige & Skoog (½MS) medium containing 0, 40 and 60 μM sodium As(III) for 20 d to observe the phenotype. Plants grown on 0 or 40 μM sodium As(III) were used to calculated seed germination rates.

For the As(III) toxicity growth assay, 3-d-old seedlings after cultivation was placed vertically on the ½MS medium containing 0, 20 or 40 μM sodium As(III) for 20 d, then the fresh weight (FW) and main root length were counted using the IMAGEJ software.

The plants for long-time arsenic treatment were grown on ½MS medium containing 20 μM sodium As(III) for 20 d and washed with distilled water three times, then dried at 65°C for > 2 d to determine the arsenic concentration.

The plants for short-time arsenic determination were grown on ½MS medium for 20 d and then transferred to the medium containing 60 μM sodium As(III) for 24 or 48 h and washed with distilled water three times, dried at 65°C for > 2 d to determine the arsenic concentration. Total arsenic content was calculated as follows: dry weight (DW) plus the arsenic concentration.

All the assays were performed on at least three biological replicates.

Determination of arsenic accumulation using ICP-MS

Yeast and plant samples for arsenic determination were dried at 80°C for 6 h and digested with a concentrated acid mixture of HNO_3, $HClO_4$ and H_2SO_4 (Guaranteed reagent, volume ratio = 4 : 1 : 0.5) at 250°C for 8 h. The concentrated acid was diluted with distilled water to the final concentration of 5%. The solution arsenic concentrations were determined using an Inductive Coupled Plasma Emission Spectrometer (ICP-OES) (iCAP6300, Thermo Electron Corp., MA, USA).

Subcellular localization of PvTIP4;1–GFP fusion protein in *P. vittata* protoplast

PvTIP4;1 was fused to *GFP* by cloning it into the 35S promoter cassette of *pGFP121* between *Xho*I and *Kpn*I restriction sites by recombination, using the following primers:

5′-ggg act cta gag gat ctc gag ATG CCT CTC CGC AAC ATT GCC CTC G-3′

5′-ttc tcc ttt acc cat ggt acc GTA GTC CTG ATC AGC AGA GGA GGG A-3′;

the constructed plasmid was named *pGFP121–PvTIP4;1*.

Incompact callus of *P. vittata* (Yang *et al.*, 2007) were used for protoplast isolation, according to the protocol described by Yoo *et al.* (2007) with modification. Enzyme solution was prepared with 20 mM MES (pH 5.7) containing 1.5% (w/v) cellulase

R10, 0.4% (w/v) macerozyme R10, 0.5% (w/v) pectolyase Y-23 (pectolyase Y-23 was used in our experiments for improvement), 0.4 M mannitol and 20 mM KCl. After the protoplasts were obtained, add 20 µl DNA (10–20 µg of plasmid DNA) and 200 µl protoplasts (*c.* 4×10^4 protoplasts) into an electroporation cuvette and mixed gently. Short pulses (3–5 s) at 700 V were delivered to the protoplast in the solution. Images of nontransfected protoplasts, control protoplasts with GFP and protoplasts with PvTIP4;1–GFP fusion protein were viewed under laser confocal scanning microscopy (Olympus FV1000MPE) after recovery at room temperature (20–25°C) for 18 h. GFP was excited at 488 nm, and the emission was detected by a photomultiplier through a 510 nm band pass filter.

Subcellular localization of the PvTIP4;1–GFP fusion protein in *P. vittata* callus

Agrobacterium strain C58 was cotransformed with the binary vector *pGFP121– PvTIP4;1* by electroporation. The *Agrobacterium* culture was used to transform the *P. vittata* gametophyte by soaking gametophytes with cuts in the *Agrobacterium* culture for 30 min. The gametophytes were dried with filter paper and transferred onto MS medium containing 0.5 mg l^{-1} 6-benzylaminopurine, 1.5 mg l^{-1} 2,4-D and 100 µM acetosyringone for 3 d at 25°C in dark. Then the gametophytes were rinsed with 300 mg l^{-1} cefradine solution 4–5 times, dried with filter paper and transferred onto MS medium containing 0.5 mg l^{-1} 6-BA, 1.5 mg l^{-1} 2,4-dichlorophenoxy, 10 mM hygromycin and 600 mg l^{-1} cefradine. After 2 wk cultivation, the gametophytes were transferred to MS medium containing 0.5 mg l^{-1} 6-BA, 1.5 mg l^{-1} 2,4-D, 15 mM hygromycin and 300 mg l^{-1} cefradine for *c.* 30 d, after which the calli of *P. vittata* were induced from gametophytes. For FM4-64 staining, the callus was transferred to 2.5 µM FM4-64 diluted in ½MS medium for 3 min. Then the fluorescent signals of both GFP and FM4-64 from the callus were observed under laser confocal scanning microscopy. GFP was excited at 488 nm, and the emission was detected by a photomultiplier through a 510 nm band pass filter. The FM4-64 was excited at 543 nm, and the emission was detected by a photomultiplier through a 581 nm band pass filter.

Preparation of total RNA and quantitative real-time PCR analysis

MIQE guidelines (Bustin *et al.*, 2009) were used to produce the data (Table S2). Two-month-old *Pteris vitatta* sporophytes were treated with 0 or 0.2 mM sodium As(III) for 24 h and total RNA was extracted from sporophytes fronds, stipes and roots tissues using the Plant RNA Reagent kit (Invitrogen) and treated with DNase using the TURBO DNA-free™ Kit (Applied Biosystems, MA, USA). All the RNA samples' quantification was detected according to the instruction. First-strand cDNAs were synthesized using *TransScript* First-Strand cDNA Synthesis SuperMix (TransGene Biotech, Beijing, China) and the water was used as no-template controls (NTCs). Real-time (RT) PCR samples were prepared with the SYBR *Premix Ex Taq*™ GC Kit (TaKaRa, CA, USA) and performed using the StepOne™ Real-Time PCR System (Applied Biosystems). *Pteris vittata Actin* and *Histon* genes were used as internal controls. The primers for quantitative (q) RT-PCR analysis were as follows, each primer pair was optimized for the amplification of a single PCR product:

PvTIP4;1 Fw: GCCAGTCTTCTGCTCAAATACACC;
PvTIP4;1 Rv: CAATACAATCTCCAGCACCAACGC;
PvActin Fw: CAGGTCCAGCCTCAGTATCG;
PvActin Rv: GCCATTCAAGCCGTTCTCT;
PvHiston Fw: GGGTTTACATTCAGCGAAGC;
PvHiston Rv GCTTTCCCTCCAGTGGACTT.

The efficiencies of all PCR reactions were between 90–100%; the limit of detection of each assay are all detected as the instruction required.

C-terminal truncated mutagenesis

C-terminal truncated mutants of PvTIP4;$1_{1\text{-}239}$ were generated on the *pAG413GAL-ccdB* vector and were transformed into the *Δfps1* yeast mutant. Yeast was diluted by sterile water to an OD_{600} of 1.0, 0.1, 0.01 and 0.001. The drop assays were performed on SD-His plates (with 2% (w/v) galactose/glucose) containing 0, 0.4 and 1.0 mM sodium As(III). The plates were incubated for 3 d at 30°C.

Site-directed mutagenesis

Site-directed mutants of *PvTIP4;1(HIAR)* was generated on the *pAG413GAL-ccdB* construct by PCR using Fast Mutagenesis System (TransGene Biotech) and the *PvTIP4;1*(*HICR*) was as controls. Then the products were transformed into the *Δfps1* and *Δacr3* yeast mutant.

For *Δfps1* yeast mutant, drop assays were performed on SD-His plates containing 0, and 0.1 mM sodium As(III) for As(III) toxicity assay and treated with 50 µM sodium As(III) in 24 h for growth curve assay. For arsenic accumulation test, yeast cells were cultured in liquid SD medium with 50 µM sodium As(III) and collected for arsenic determination.

For *Δacr3* yeast mutant, drop assays were performed on SD-His plates containing 0, and 0.1 mM sodium As(V) for As(V) toxicity assay and treated with 50 µM sodium As(V) in 24 h for growth curve assay. For arsenic accumulation test, yeast cells were cultured in liquid SD medium with 50 µM sodium As(V) and collected for arsenic determination.

Homology modelling of PvTIP4;1

PvTIP4;1(HICR) and PvTIP4;1(HIAR) three-dimensional models were constructed using the MODELLER software (Fiser & Sali, 2003). A high-resolution aquaporin structures *E. coli* GlpF (PDB ID: 1FX8) were used as templates simultaneously in the comparative modelling procedure. To analysis the pore dimensions of PvTIP4;1, structural models was carried out using the program MOLE v.2.0 (Sehnal *et al.*, 2013), which is a universal toolkit for rapid and fully automated location and characterization of channels, tunnels and pores in protein structures. Dijkstra's algorithm

is used to identify tunnels as the shortest paths between the start and end points. Three-dimensional models and the analyses of pores were visualized within PyMOL (DeLano & Lam, 2005).

Results

The isolation of *PvTIP4;1* gene and sequence analysis

To identify As(III) uptake genes in *P. vittata*, the As(III)-resistant yeast strain *Δfps1* was transformed with a cDNA expression library generated from *P. vittata*. Gene expression from the GAL1 promoter in *pAG413GAL* vector is induced by galactose, but repressed by glucose. A transformed yeast colony F7 was sensitive to 1 mM As(III) under which the growth of *Δfps1* was not affected (Fig. 1).

Details of the insert fragment of F7 were deposited into GenBank (accession no. KC517114); it encodes an aquaporin similar in sequence to the yeast *Fps1* gene. The coding region corresponded to a 260 amino acid polypeptide, which was predicted by hydropathy analysis to have six bilayer-spanning domains. The six membrane-spanning domains are interrupted by five loops (loops A–E), and cytosolic N- and C-terminal extensions. Loops B and E contain the highly conserved asparagine–proline–alanine (NPA) boxes and four residues from helix 2 (H2), helix 5 (H5), and loop E (LE1 and LE1) form the Ar/R region (Fig. 2a).

Protein blast on NCBI showed that the coding sequence (CDS) of F7 encodes a protein similar in sequence to MIPs. Phylogenetic analysis of this protein with MIPs from the moss *P. patens*, dicot *A. thaliana* and monocot *O. sativa* shows that the aquaporin belongs to a tonoplast intrinsic protein (TIP) subfamily (Fig. 2b). Further detailed analysis of TIPs indicates that it is a TIP4s protein (Fig. 2c) and therefore the protein was christened 'PvTIP4;1'.

Functional analyses of the PvTIP4;1 protein in yeast

To confirm the As(III) sensitivity observed in plate assay, the growth of *Δfps1* expressing *PvTIP4;1* was also monitored in liquid culture. Expression of *PvTIP4;1* induced by galactose caused growth retardation in *Δfps1*, either treated with 100 μM As(III) or not (Fig. 3a). However, the growth of *Δfps1* carrying empty vector was slightly affected by 100 μM As(III), whereas *Δfps1* expressing *PvTIP4;1* was significantly inhibited at various times (Fig. 3a). The relative growth comparing 100 μM As(III) treatment with no arsenic control unambiguously showed that PvTIP4;1 transformants were much more sensitive to As(III), with a growth reduction of *c.* 50% compared with *c.* 5% of vector control after 24 h cultivation (Fig. 3b). These results demonstrate that PvTIP4;1 reverses As(III) resistance of *Δfps1* cells, which is coincident with the results of the plate assay (Fig. 1). Under 100 μM As(III) exposure conditions, whole cell As uptake revealed that *Δfps1* expressing *PvTIP4;1* accumulated much more As time periods compared with *Δfps1* carrying the empty vector after 0, 0.5, 1 or 2 h (Fig. 3c). Under short-term (0.5 h) As(III) exposure, expression of *PvTIP4;1* caused enhanced As accumulation in an As(III) dose-dependent manner (Fig. 3d). Together, expression of *PvTIP4;1* caused increased As accumulation over time or with As(III) supply, achieving approximately four- to six-folds higher than the vector control (Fig. 3c,d). These results indicated that PvTIP4;1 may acts as an As(III) uptake channel in yeast.

We expressed PvTIP4;1 in As(V) sensitive *Δacr3* yeast mutant, which is the deletion of yeast As(III) antiporter on plasma membrane. This mutant lacks efflux transporter for As(III) and, as the result of the activity of As(V) reductase Acr2p, accumulates As (III) in the presence of externally supplied As(V). When 200 μM As(V) was added, expression of PvTIP4;1 in *Δacr3* rendered cells more resistant toward to externally supplied As(V) compared with vector control (Fig. 4a,b), indicating that PvTIP4;1 enhanced As(V) tolerance of *Δacr3*. The relative growth showed that PvTIP4;1 greatly promoted the growth of *Δacr3* under As (V) stress (Fig. 4c). Transport assays revealed that expressing PvTIP4;1 significantly reduced arsenic accumulation over prolonged 100 μM As(V) exposure (Fig. 4d). Cells expressing PvTIP4;1 also showed decreased arsenic accumulation after exposure to various amounts of As(V) supplied for 24 h (Fig. 4e).

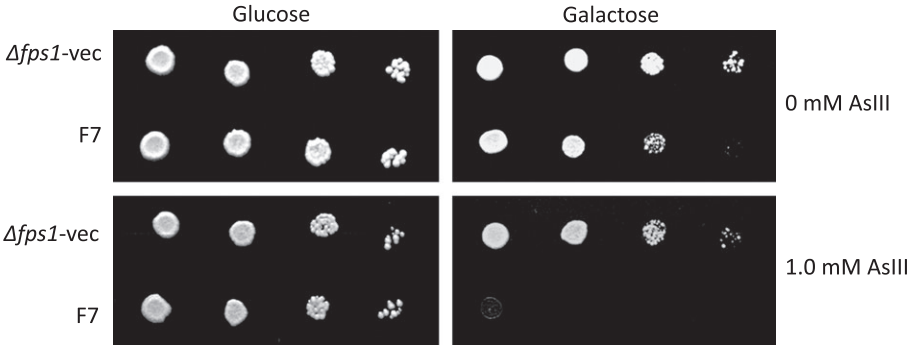

Fig. 1 A transformed yeast colony F7 was found to be sensitive to 1 mM arsenite (As (III)). *Saccharomyces cerevisiae Δfps1* was transformed with either *pAG413GAL* (empty vector) or with *pAG413GAL* containing *Pteris vittata* cDNA. Yeast transformants were grown in synthetic defined (+2% glucose-His) medium containing glucose or galactose and with or without 1 mM As(III). Plates were incubated for 3 d at 30°C. Drop tests were repeated at least three times with similar results.

Fig. 2 PvTIP4;1 is a tonoplast intrinsic protein (TIP) subfamily aquaporin. (a) The predicted topology of PvTIP4;1 protein. The conserved motif asparagine–proline–alanine (NPA) (stars) and aromatic/arginine (Ar/R) selectivity filter residues H2, H5, LE1 and LE2 (diamonds) are indicated. (b) Neighbour-joining phylogenetic relationship of PvTIP4;1 with MIP proteins. Aquaporins related to As(III) transport are indicated by black circles. XIPs, uncategorized X intrinsic proteins; PIPs, plasma membrane intrinsic proteins; GIPs, GlpF-like intrinsic proteins; SIPs, small basic intrinsic proteins; NIPs, nodulin-26 like intrinsic proteins. The abbreviations of plant names are as follows: At, *Arabidopsis thaliana*; Os, *Oryza sativa*; Pp, *Physcomitrella patens*; Pv, *Pteris vittata*; Zm, *Zea mays.* (c) Neighbour-joining phylogenetic relationship of PvTIP4;1 with TIP proteins of plants.

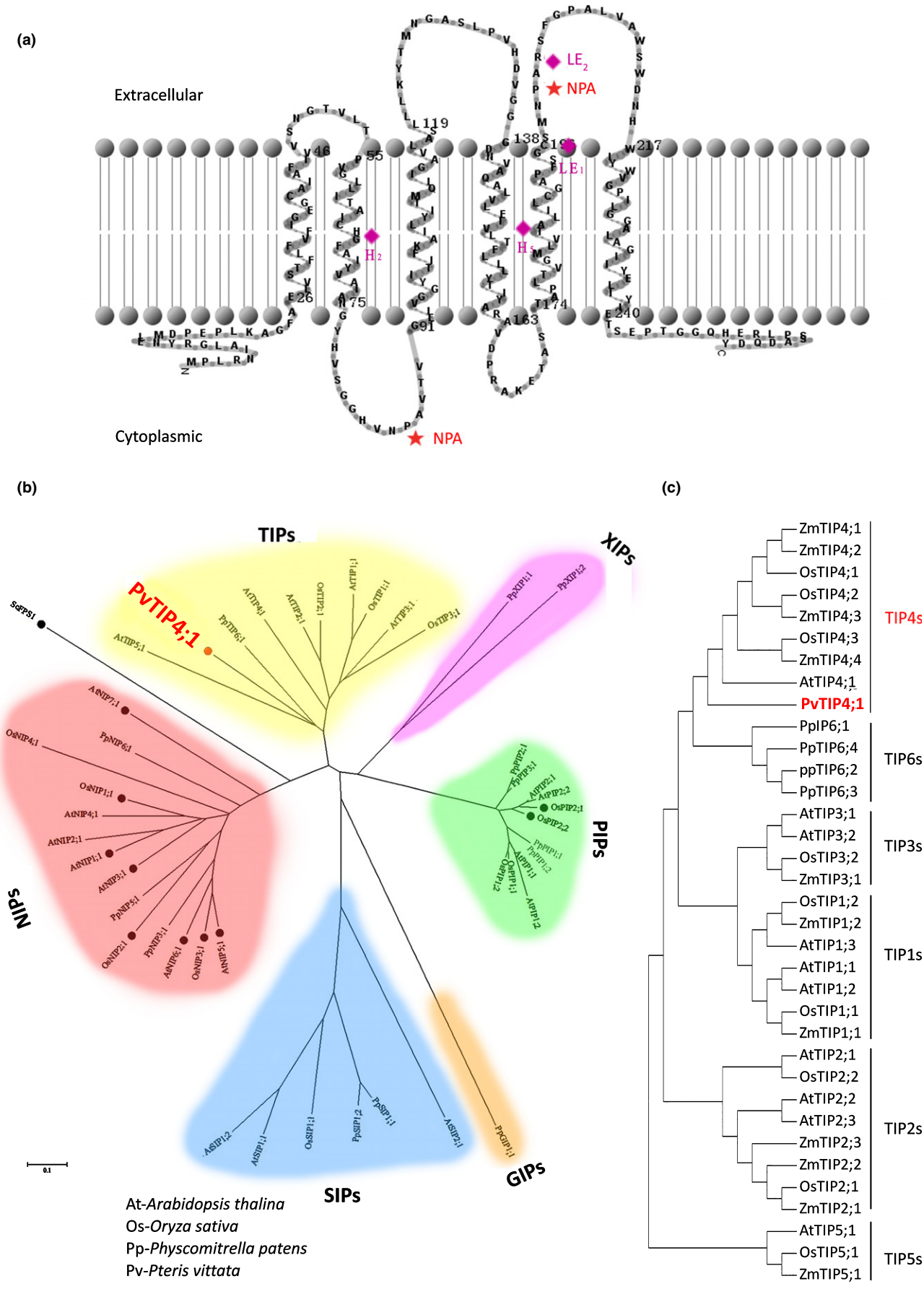

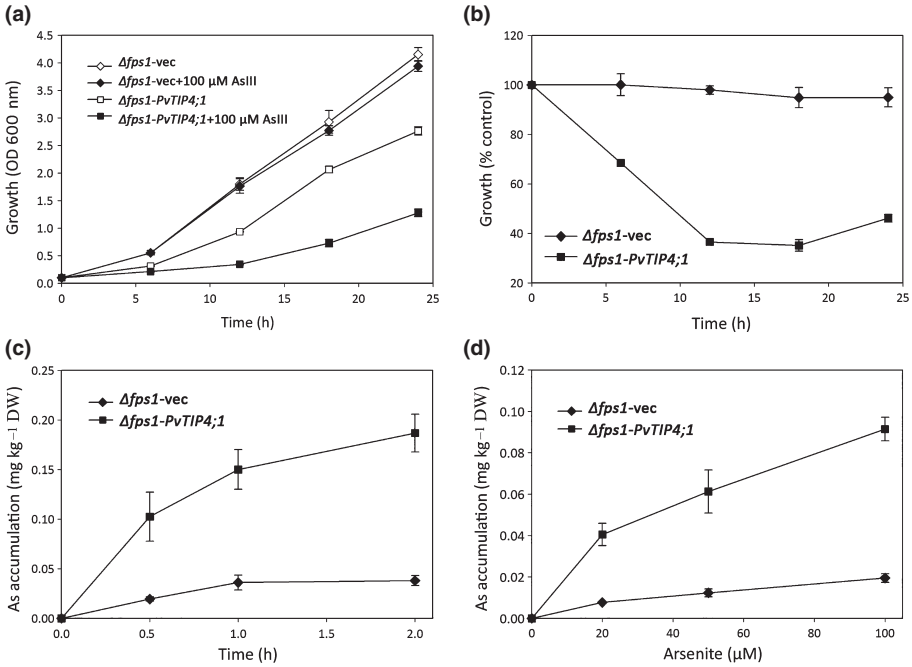

Fig. 3 Expressing *PvTIP4;1* sensitizes yeast mutant *Δfps1* to arsenite (As(III)) by increasing arsenic (As) accumulation. (a) Growth curves of *Δfps1* transformed with empty vector (diamonds) and *Δfps1* expressing *PvTIP4;1* (squares) yeast cultivated in liquid synthetic defined (+ 2% galactose-His) culture or culture containing 100 μM As(III) and the values of OD_{600} of the mediums were tested. (b) Relative growth curves of the values of OD_{600} of *Δfps1* (diamonds) and *Δfps1* expressing *PvTIP4;1* (squares) yeast under 100 μM As (III) compared to control. (c) Arsenic accumulation in *Δfps1* (diamonds) and *Δfps1* expressing *PvTIP4;1* (squares) yeast cultured in 100 μM As(III) for 0.5, 1 and 2 h. (d) Arsenic accumulation in *Δfps1* (diamonds) and *Δfps1* expressing PvTIP4;1 (squares) yeast cultured in 20, 50, 100 μM As(III) for 0.5 h. Error bars, mean ± SE. OD, optical density.

Based on our transport and growth data, we showed that PvTIP4;1 mediates As(III) efflux and influx in the yeast which supports the notion that PvTIP4;1 is a bi-directional channel. The results of the yeast system demonstrated that PvTIP4;1 is able to facilitate the diffusion of the As(III) substrate.

Functional analyses of the PvTIP4;1 protein in *A. thaliana*

PvTIP4;1 cDNA was heterogeneously expressed in *A. thaliana* under the control of CaMV-35S promoter to characterize its role in plant. Plant RNAs were isolated and RT-PCR analyses using gene-specific primers indicated that the transgene was expressed in L9 and L27 with no detectable transcripts in the wild-type (Fig. S1a). When seeds germinated on the medium containing 0, 40 or 60 μM As(III), the seed germination rate of transgene *Arabidopsis* was decreased by 60% under 40 μM As(III) treatment (Fig. S1b,c). To test the As(III) sensitivity phenotypes, seeds of *Arabidopsis* untransformed control and the two independent transgenic lines overexpressing *PvTIP4;1* were grown for 20 d on 1/2 MS medium containing 0, 20 and 40 μM As(III). There were no obvious phenotypic differences between transgenic lines and wild-type (WT) control plants grown on media without As(III). However, growth of both shoots and roots of the transgenic lines expressing *PvTIP4;1* was more severely stunted than that of WT plants on media supplemented with 20 and 40 μM As(III) (Fig. 5a). The fresh shoot biomass of the PvTIP4;1 transgenic lines L9 and L27 had dropped by 80% compared with the control, whereas the wild-type controls dropped by only 50% (Fig. 5b). The main root length of the *PvTIP4;1* transgenic lines was 50% that of the WT controls (Fig. 5c). To examine the transport activity of *PvTIP4;1 in vivo*, we measured As accumulation in the *PvTIP4;1* transgenic lines L9 and L27. The transgenic plants were grown vertically on plates containing 20 μM As(III) for 20 d, and As concentration in the whole plant was measured by ICP-MS. As shown in Fig. 5(d), As accumulations in L9 and L27 were significantly higher than those in WT plants.

For the short-term kinetic uptake studies, *PvTIP4;1* transgenic lines L9 and L27 and the WT controls were grown on the plates without As(III) for 20 d and then transferred to the medium containing 60 μM sodium As(III) for 24 and 48 h. According to the Fig. 5(e), there were no obvious growth reduction phenotypes between the transgenic lines and the WT controls. The As concentration and content in whole plant showed that the transgenic lines L9 and L27 absorbed more arsenic than the WT controls (Fig. 5f, g), demonstrating that *PvTIP4;1* is capable of transporting As(III).

Subcellular localization of PvTIP4;1

TIPs may have a more complex subcellular distribution in plant (Wudick *et al.*, 2009). In order to evaluate the subcellular location of PvTIP4;1, we first used the subcellular localization prediction software PSORT to predict (Nakai & Horton, 1999). The software predicted that the most possible location of PvTIP4;1 was plasma membrane and may also be chloroplast thylakoid membrane, the Golgi body or the endoplasmic reticulum membrane (Table S3).

To confirm the prediction, GFP-fused PvTIP4;1 was expressed in *P. vittata* protoplasts and callus. PvTIP4;1 was C terminally linked to GFP, and expression of the fusion proteins was driven by a 35S promoter. Protoplasts transformed by the empty plasmid pGFP121 carrying GFP alone served as control. GFP fluorescence of PvTIP4;1 tagged constructs in protoplasts was confined to a ring in the protoplasts (Fig. 6), while GFP alone was confined in nuclear and cytoplasm internal structures but

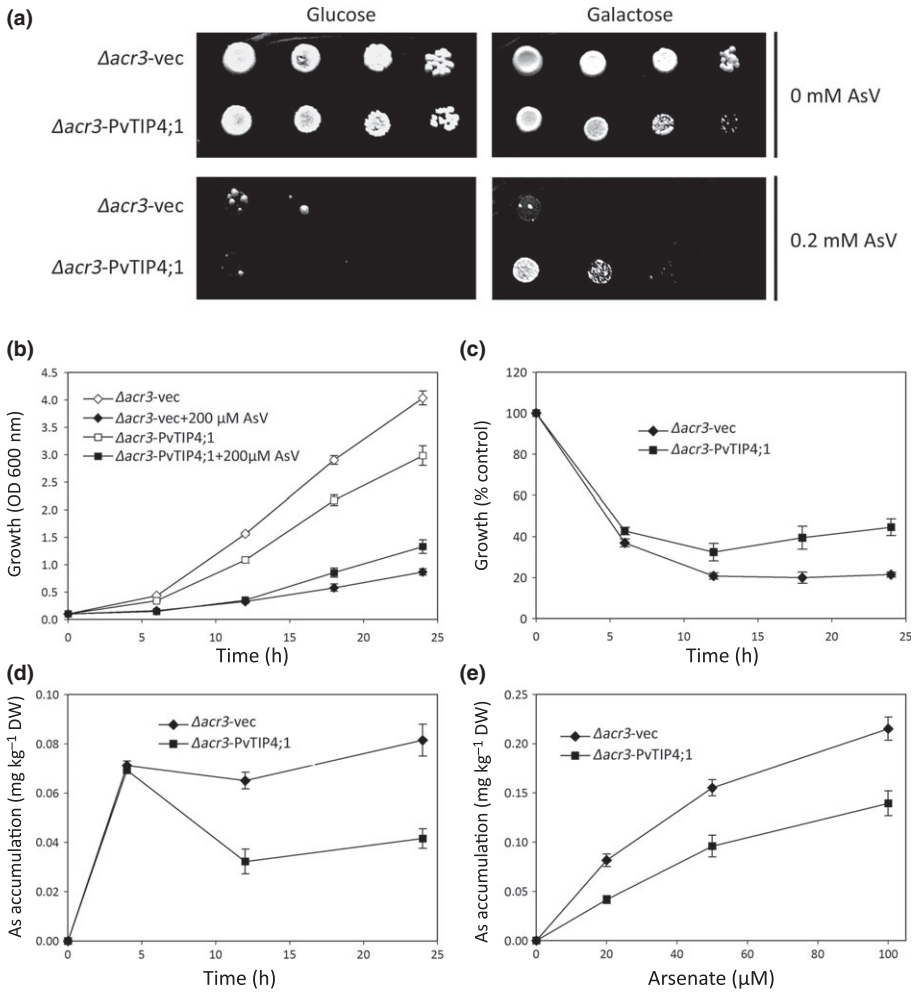

Fig. 4 Expressing *PvTIP4;1* enhances arsenate (As(V)) tolerance in yeast mutant *Δacr3* by decreasing arsenic (As) accumulation. (a) *Saccharomyces cerevisiae Δacr3* was transformed with either pAG413GAL (empty vector) or with pAG413GAL containing PvTIP4;1 CDS. Yeast transformants were grown in synthetic defined (SD) (+2% glucose-His) medium containing glucose or galactose and with or without 0.2 mM As(V). Plates were incubated for 5 d at 30°C. Drop tests were repeated at least three times with similar results. (b) Growth curves of *Δacr3* transformed with empty vector (diamonds) and *Δacr3* expressing *PvTIP4;1* (squares) yeast cultivated in liquid SD (+2% galactose-His) culture or culture containing 0.2 mM As (V) and the values of OD_{600} of the mediums were tested. (c) Relative growth curves of the values of OD_{600} of *Δacr3* (diamonds) and *Δacr3* expressing *PvTIP4;1* (squares) yeast under 0.2 mM As(V) compared to the No As control. (d) Arsenic accumulation in *Δacr3* (diamonds) and *Δacr3* expressing *PvTIP4;1* (squares) yeast cultured in 100 μM As(V) over time. (e) Arsenic accumulation in *Δacr3* (diamonds) and *Δacr3* expressing *PvTIP4;1* (squares) yeast cultured in varying concentrations of As(V) for 24 h. Error bars, mean ± SE; CDS, coding sequence; OD, optical density.

was excluded from the vacuolar lumen. This suggested that PvTIP4;1 may localize to the plasma membrane in *P. vittata*.

GFP fluorescence alone was observed in nuclear and cytoplasm internal structures (Fig. 7a), whereas fluorescence due to the PvTIP4;1–GFP fusion proteins was localized in the periphery of the callus cells (Fig. 7b). The transgenic callus cells were also stained with the plasma membrane marker FM4-64 and red fluorescence labeling of the plasma membrane was observed (Fig. 7b). GFP and red fluorescence signals overlapped (Fig. 7b). The image resolution and FM4-64 staining suggested that PvTIP4;1 localized to the plasma membrane in *P. vittata*.

Tissue specificity of *PvTIP4;1* expression

MIQE guidelines (Bustin *et al.*, 2009) were used to produce the data (Table S2). The levels of *PvTIP4;1* mRNA in different tissues were quantified by qRT-PCR to study the expression pattern of *PvTIP4;1* gene in *P. vittata* sporophytes. The results showed that the transcripts of *PvTIP4;1* were accumulated at relatively high levels in roots, whereas its expression level was relatively low in stipes and fronds (Fig. 8a–c). Under As(III) treatment, the abundance of *PvTIP4;1* transcripts varied little in stipes, fronds and roots (less than two-fold) compared with the No As control (Fig. 8b,c), suggesting that As(III) may have little effect on expression activity of PvTIP4;1.

Influence of the C-terminal of PvTIP4;1 on arsenic transport

Comparison of PvTIP4;1 and TIP4s in plants revealed that C-terminus of PvTIP4;1 are much longer than that of TIP4s in *A. thaliana* (Fig. 9). It was previously reported that, hydrophilic N-terminal or C-terminal domain is necessary for NIPs to get functional expression in yeast (Bienert *et al.*, 2008). Therefore, we genetically engineered PvTIP4;1 with different C-terminal domain versions including PvTIP4;1, PvTIP4;$1_{1\text{-}239}$ and expressed them in As(III)-resistant *Δfps1* yeast mutant. Yeast transformants were plated on medium containing 0, 0.4 and 1 mM As(III) with glucose or galactose. Growth comparing As (III) treatment with No As(III) control showed no difference with PvTIP4;1. The C-terminus had little impact on arsenic sensitivity of PvTIP4;1 (data not shown).

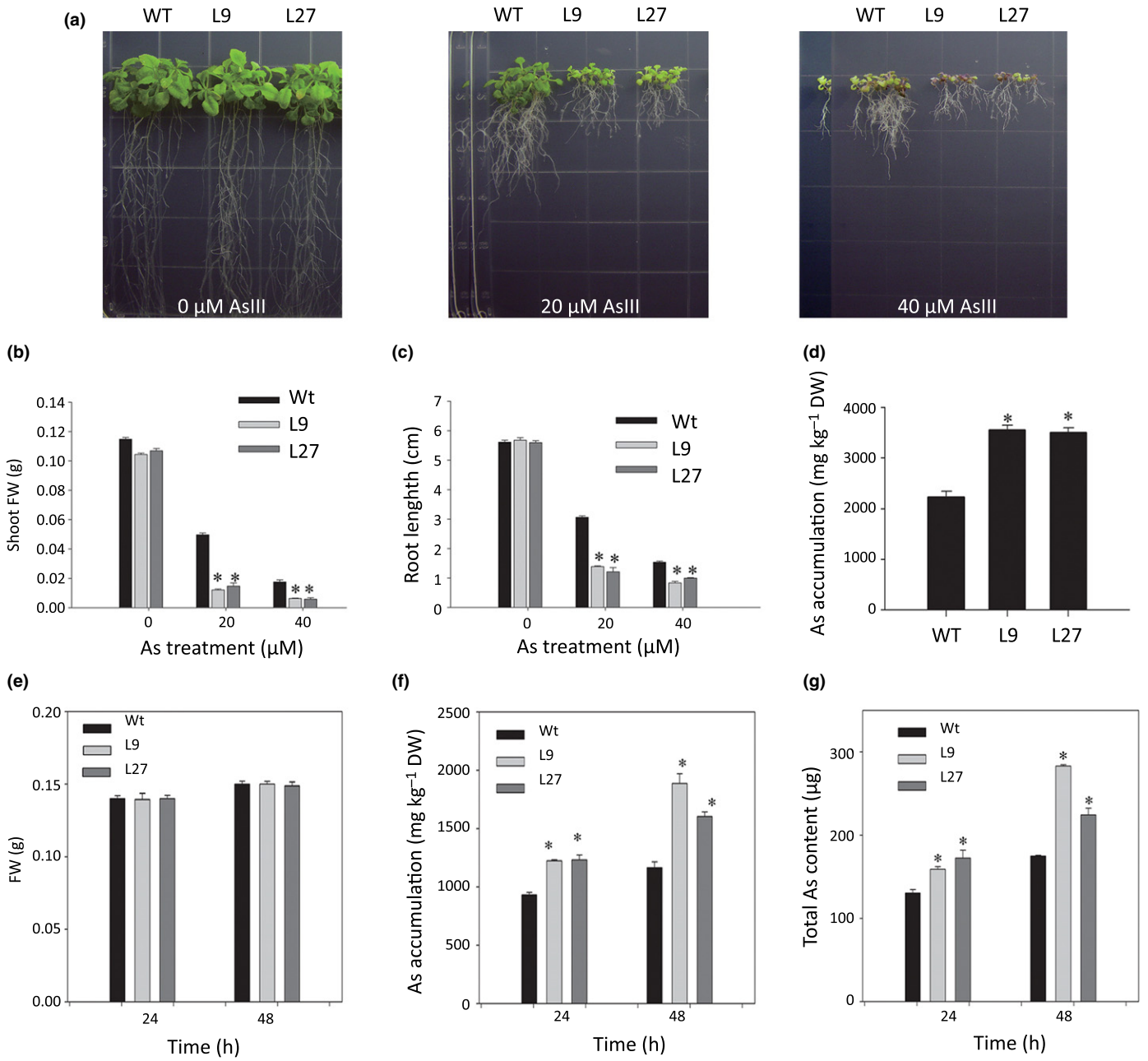

Fig. 5 Arsenic (As) toxicity and accumulation of transgenic *Arabidopsis* plants expressing *PvTIP4;1* in long time and short time. (a) Comparative growth of 3-d-old *Arabidopsis* seedlings grown vertically on plates with 0, 20, and 40 μM arsenite (As(III)) for 10 d. (b, c) Statistical analyses of (b) FW and (c) main root length of 3-d-old seedlings of wild-type (WT, black bars), L9 (white bars), and L27 (grey bars) after cultivation under 0, 20 and 40 μM As(III) concentrations for 20 d ($n = 10$ plants per treatment per line). (d) Arsenic accumulation in *PvTIP4;1* transgenic *Arabidopsis* plants under 20 μM As(III) treatments. Asterisks indicate significant differences from the WT detected by one-way analysis of variance (ANOVA) (*, $P < 0.05$). Error bars, mean ± SE. (e) Statistical analyses of FW of 20-d-old seedlings of WT (black bars), L9 (white bars), and L27 (grey bars) after cultivation under 60 μM As(III) concentration for 24 and 48 h ($n = 10$ plants per treatment per line). (f) Arsenic accumulation in *PvTIP4;1* transgenic *Arabidopsis* plants under 60 μM As(III) treatments for 24 and 48 h. (g) Total arsenic content in *PvTIP4;1* transgenic *Arabidopsis* plants under 60 μM As(III) treatments for 24 and 48 h. Asterisks indicate significant differences from the WT detected by one-way analysis of variance (ANOVA) (*, $P < 0.05$). Error bars, mean ± SE.

The role of cysteine in LE1 of PvTIP4;1 Ar/R domain on arsenic transport

It has also been proposed that the Ar/R region serves as a selectivity filter for the transport of substrates. Interestingly, the Ar/R domain of PvTIP4;1 consists of a cysteine in LE1 which is different from all other Ar/R filters of TIPs in MIPModDB (http://bioinfo.iitk.ac.in/MIPModDB/index.html) (Fig. 9; Table 1). To investigate whether the special Ar/R domain could influence the arsenic transport activity, we substituted alanine which is normal in other TIPs for cysteine in LE1 and expressed it in *Δfps1* and *Δacr3* yeast mutants. As is shown in Fig. 10(a)

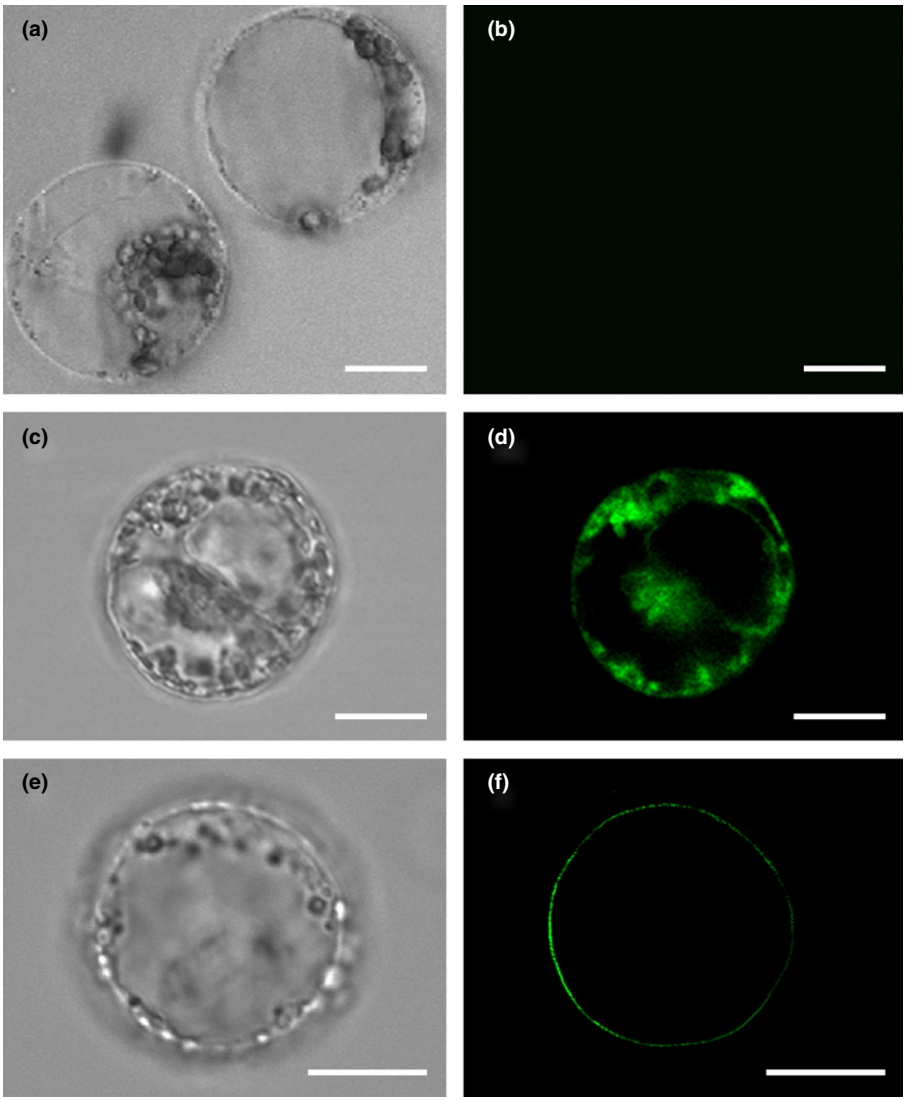

Fig. 6 Subcellular localization of GFP-fused PvTIP4;1 in protoplast of *Pteris vittata*. (a) Transmission image of nontransfected protoplasts. (b) Green fluorescent protein (GFP) fluorescence image of nontransfected protoplasts. (c) Transmission image of protoplasts transformed with GFP alone. (d) GFP fluorescence image of protoplasts transformed with GFP alone. (e) Transmission image of protoplasts transformed with PvTIP4;1–GFP. (f) GFP fluorescence image of protoplasts transformed with PvTIP4;1–GFP. Bars, 10 μm.

and (b), the growth of *Δfps1* yeast mutant with native PvTIP4;1 (HICR) is inhibited on the medium containing 0 and 100 μM As(III), while site-directed mutation at the LE1 (selectivity filter HIAR) grew better. Transport assays also revealed that the site-directed mutation of PvTIP4;1 resulted in *c.* 10% reduction in its arsenic transport activity when treated with 50 μM As(III) for 24 h (Fig. 10c). Expression of PvTIP4;1(HIAR) and PvTIP4;1 (HICR) in *Δacr3* showed that the mutant expressing PvTIP4;1 (HIAR) was more sensitive than the PvTIP4;1(HICR) and caused an *c.* 13% increased As accumulation when treated with As(V) for 24 h (Fig. 10a,d,e).

A homology model was produced for PvTIP4;1 (HICR) and PvTIP4;1 (HIAR) by alignment with the GlpF structures followed by three-dimensional model building. That the α-carbon backbone of PvTIP4;1 (HICR) and PvTIP4;1 (HIAR) model shows a reasonable overall similarity with the GlpF experimental structures within the membrane-spanning helices and loops (Fig. S2) guaranteed the validity of the modelling protocol. When viewed perpendicular to the plane of the membrane, the Ar/R regions of PvTIP4;1 (HIAR) reveals significant differences from PvTIP4;1 (HICR) structures (Fig. 11a). Comparison of the PvTIP4;1 (HICR) and PvTIP4;1 (HIAR) Ar/R regions suggests that the replacement of cysteine PvTIP4;1 (HICR) with alanine at LE1 results in a more narrower Ar/R region (Fig. 11b). This is supported by analysis of the predicted pore architecture of the PvTIP4;1 models using MOLE, which shows that the diameter at Ar/R regions of PvTIP4;1 (HICR) is wider than that of PvTIP4;1 (HIAR) (Fig. 11c red arrow). Moreover, PvTIP4;1 (HIAR) showed another aperture (Fig. 11c blue arrow) which is more narrow than that of the Ar/R region of PvTIP4;1 (HICR).

Discussion

Arsenic is a highly toxic metalloid that commonly occurs in the form of inorganic As(III) and As(V) (Kaur *et al.*, 2011). In aerobic soils, As(V) is the dominant form of arsenic (Meharg & Hartley-Whitaker, 2002) and can be reduced to As(III) due to the

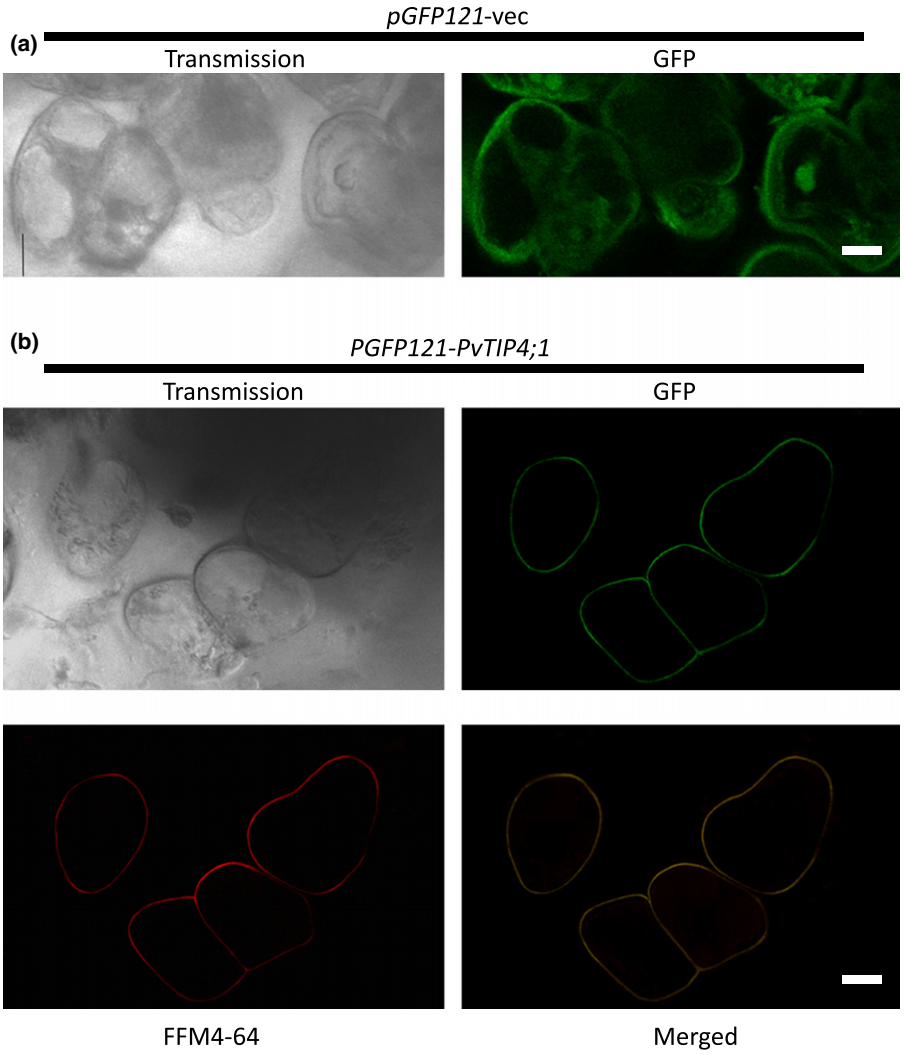

Fig. 7 Subcellular localization of GFP-fused PvTIP4;1 in callus of *Pteris vittata*. (a) Green fluorescent protein (GFP) control bright and fluorescence field. (b) PvTIP4;1–GFP bright field, fluorescence field, FM4-64 staining and the merged image of GFP and FM4-64. Bars, 10 μm.

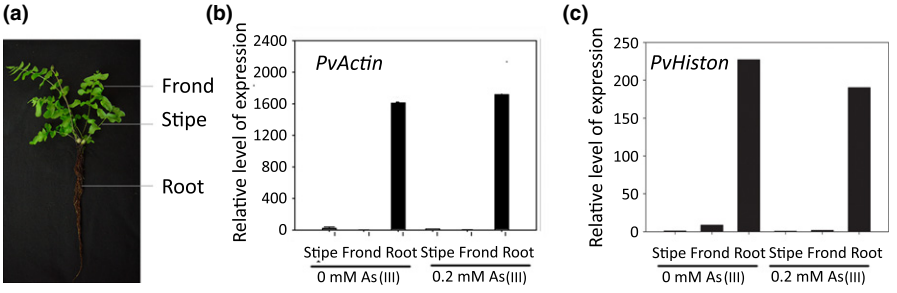

Fig. 8 Tissues expression of *PvTIP4;1* in *Pteris vittata* sporophyte. (a) The stipe, frond and root of *P. vittata*. (b, c) Expression of *PvTIP4;1* in *P. vittata* sporophyte tissues. (b) *PvActin* was used as the control and (c) *PvHiston* was used as the control. Each bar indicates the fold change in the expression of *PvTIP4;1* in stipe, frond and root of plants grown in 0.2 mM arsenite (As(III)) for 24 h relative to plants grown in the absence of arsenic.

microbial activity in the rhizosphere (Macur *et al.*, 2001). Consequently, *P. vittata* encounters a mixed pool of As(V) and As(III) in aerobic environment and *P. vittata* can directly absorb As(III) from growth medium (Wang *et al.*, 2011). As(III) uptake is important for the high efficiency of arsenic assimilation, which is the prerequisite for arsenic hyperaccumulation.

However, little information is known about the mechanism utilized by *P. vittata* in the uptake of As(III). In bacteria, yeast and humans, some aquaglyceroporins including *E. coli* glycerol facilitator GlpF (Meng *et al.*, 2004), the yeast glycerol channel protein Fps1p (Wysocki *et al.*, 2001), and the mammalian aquaglyceroporins AQP7 and AQP9 (Liu *et al.*, 2002), can transport As(III). Members of plant aquaporins in *Arabidopsis thaliana* and *Oryza sativa* also showed the ability to carry out As (III) uptake (Bienert *et al.*, 2008; Isayenkov & Maathuis, 2008; Ma *et al.*, 2008; Kamiya *et al.*, 2009; Mosa *et al.*, 2012). To identify As(III) uptake genes in *P. vittata*, we constructed a *P. vittata* cDNA expression library and transformed it into the As(III)-resistant yeast strain *Δfps1*. Excitingly, a new aquaporin protein was identified (Fig. 1) from a sensitive transformant and the

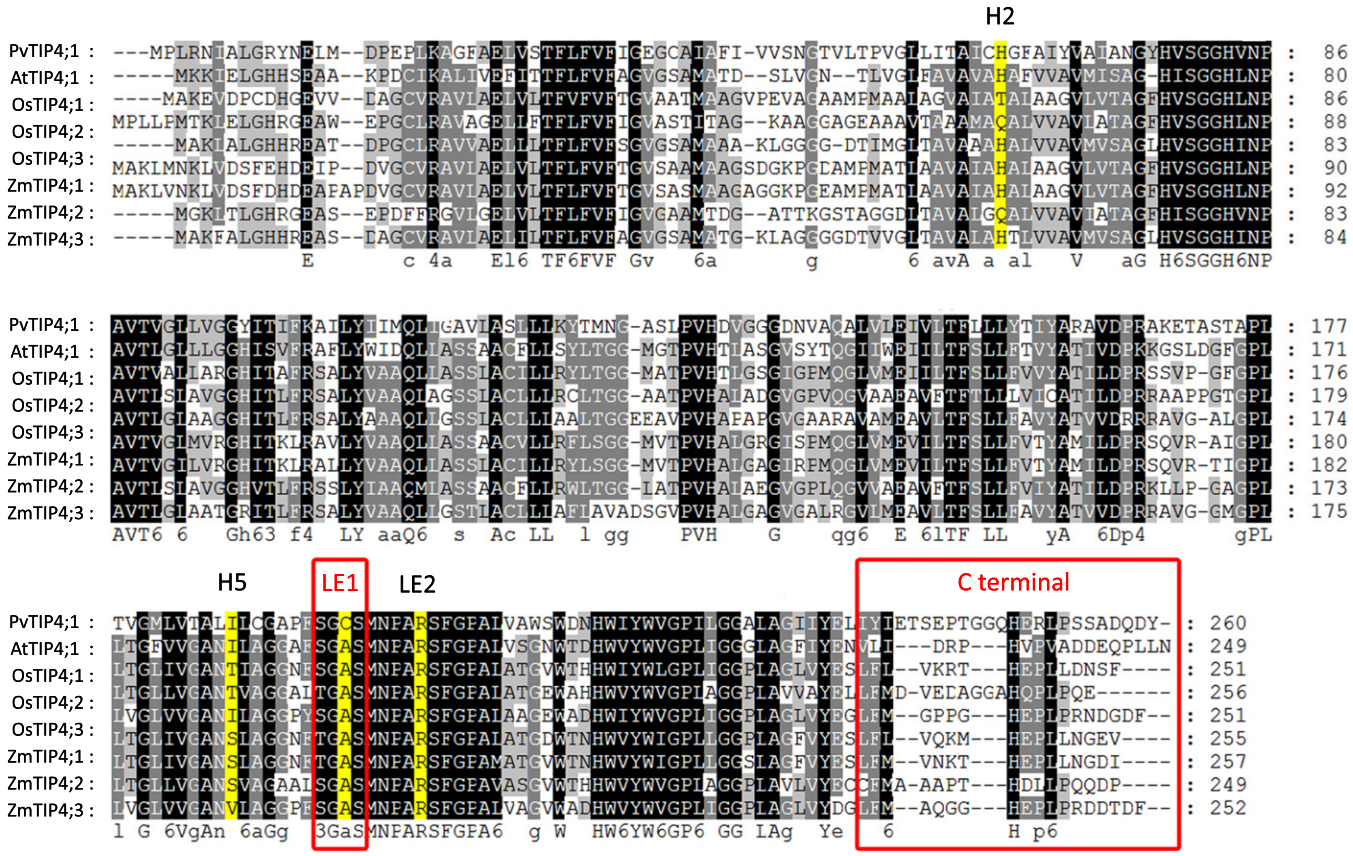

Fig. 9 Comparison of the amino acid sequence of PvTIP4;1 with the known TIP4s proteins in plant. Amino acid sequences are aligned by GeneDoc software. Four residues of aromatic/arginine (Ar/R) selectivity filter are highlighted in yellow. The C-terminus region and Ar/R selectivity filter residues LE1 are shown in red boxes.

Table 1 Aromatic/arginine (Ar/R) signatures of TIP4s from *Pteris vittata*, *Arabidopsis*, rice and maize

	Ar/R			
TIP4 Members	H2	H5	LE1[a]	LE2
PvTIP4;1	H	I	C[b]	R
OsTIP4;3, AtTIP4;1	H	I	A	R
ZmTIP4;4	H	V	A	R
ZmTIP4;1, ZmTIP4;2	H	S	A	R
OsTIP4;2	Q	T	A	R
ZmTIP4;3	Q	S	A	R
OsTIP4;1	T	T	A	R

[a]LE1 residues are shown under the grey background.
[b]The LE1 residue in PvTIP4;1 is shown in red.

phylogenetic analysis showed that it is a plant TIP homologue, with a very high similarity to TIP4s (Fig. 2) and therefore the protein was named 'PvTIP4;1'.

We assayed the As(III) toxicity of *PvTIP4;1* in yeast and *A. thaliana*. The relative growth showed that *PvTIP4;1* transformants were much more sensitive to As(III) than *Δfps1* carrying empty vector (Fig. 3a,b). Expression of *PvTIP4;1* caused more As accumulation than the vector control (Fig. 3c,d). Moreover, *PvTIP4;1* also confers As(V) tolerance in *Δacr3* yeast cells (Fig. 4) and likely functions as an As(III) effluxer based on its ability to suppress the arsenic accumulation phenotypes of *Δacr3* yeast. The fact that *PvTIP4;1* acts as a bi-directional As(III) transporter is similar with some former reported aquaporins of NIPs from *A. thaliana*, *O.* and *L. japonicas* and Fps1p from yeast.

To further investigate the function of *PvTIP4;1* in plants, *PvTIP4;1* cDNA was heterogeneously expressed in *A. thaliana*. The seed germination rate of transgene *Arabidopsis* was decreased (Fig. S1b,c) on the As(III) medium. After growth for 20 d under As(III) condition, the growth of both shoots and roots of the transgenic lines expressing *PvTIP4;1* was more severely hindered than that of the WT plants on As(III) media (Fig. 5a–c) and As concentrations in the L9 and L27 were significantly higher than those in WT plants (Fig. 5d). As the transgenic lines were severely stressed, the absolute uptake of arsenic was difficult to be estimated. To calculate the total uptake of arsenic in WT, L9 and L27, the short-term kinetic uptake studies were performed. The data showed that L9 and L27 can absorb more arsenic than the WT plants (Fig. 5e–g). Heterologous expression in *Arabidopsis* demonstrated that *PvTIP4;1* facilitates arsenic accumulation and induced arsenic sensitivity.

To further understand the function of the *PvTIP4;1* gene, we studied the subcellular and tissue localization of PvTIP4;1. TIP is tonoplast intrinsic protein for short and was originally found in tonoplasts (Johnson *et al.*, 1989, 1990). Subsequent research showed that TIPs may have a more complex subcellular

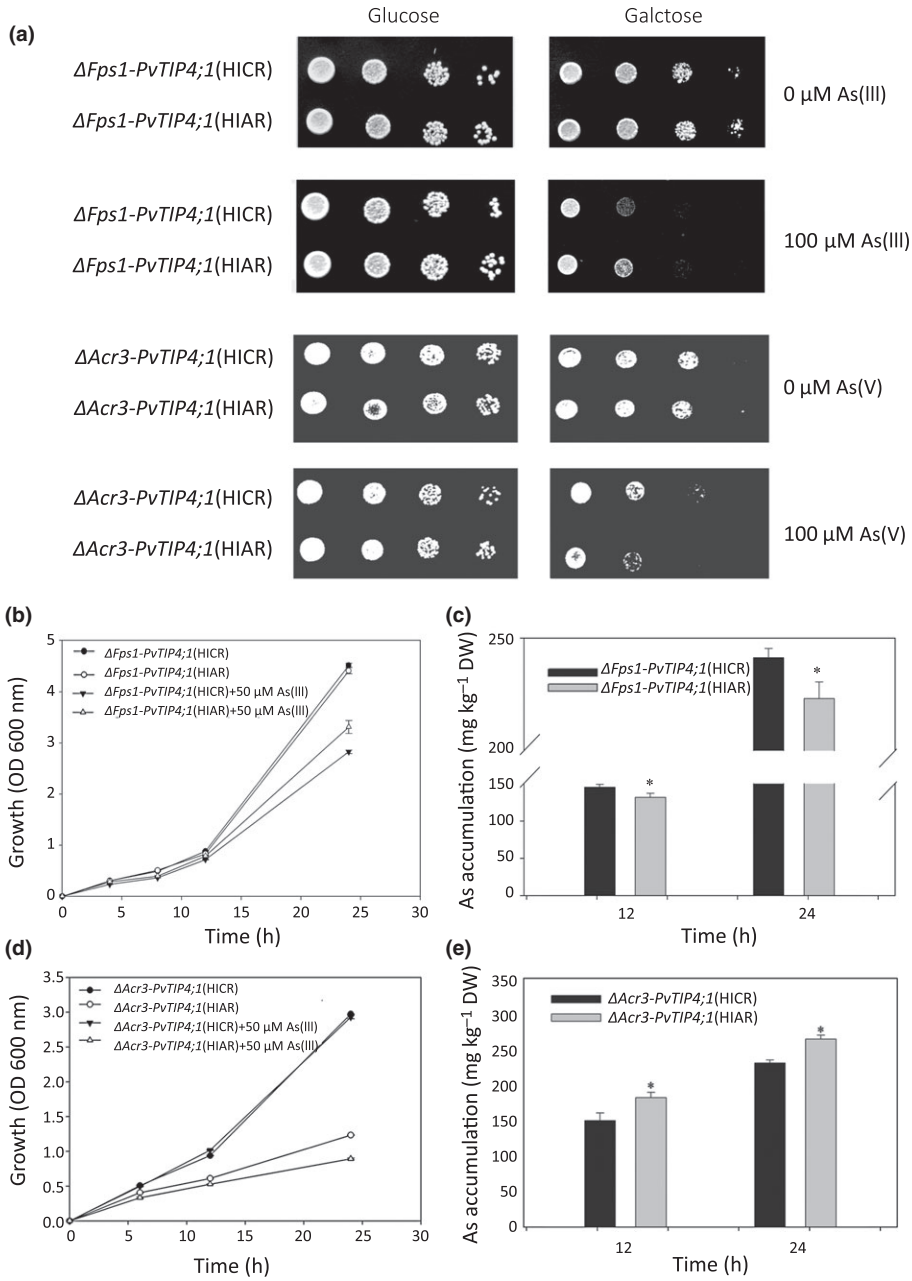

Fig. 10 Influence of aromatic/arginine (Ar/R) selectivity filter substitution of PvTIP4;1 on the transport activity for arsenic (As) in *Δfps1* and *Δacr3*. (a) *Saccharomyces cerevisiae Δfps1* and *Δacr3* were transformed with *pAG413GAL-PvTIP4;1* (HICR), and *pAG413GAL-PvTIP4;1*(HIAR) respectively. Yeast transformants were grown in synthetic defined (SD) (+2% glucose-His) medium containing glucose or galactose and with or without 100 μM arsenite (As(III)) and 100 μM arsenate (As (V)). Plates were incubated for 3 d at 30°C. Drop tests were repeated at least three times with similar results. (b) Growth curves of *Δfps1* transformed with *PvTIP4;1*(HICR) (closed) and *PvTIP4;1*(HIAR) (open), cultivated in liquid SD (+2% galactose-His) culture containing 50 μM As(III) for 24 h. The values of OD_{600} of the mediums were tested. (c) Arsenic accumulation in *Δfps1* expressing *PvTIP4;1*(HICR) (solid) and *PvTIP4;1*(HIAR) (hollow) cultured in 50 μM As(III) for 12 h and 24 h. (d) Growth curves of *Δacr3* transformed with *PvTIP4;1*(HICR) (solid) and *PvTIP4;1*(HIAR) (hollow), cultivated in liquid SD (+2% galactose-His) culture containing 50 μM As(V) for 24 h. The values of OD_{600} of the mediums were tested. (e) Arsenic accumulation in *Δacr3* expressing *PvTIP4;1* (HICR) (solid) and *PvTIP4;1*(HIAR) (hollow) cultured in 50 μM As(V) for 12 and 24 h. Asterisks indicate significant differences detected by one-way analysis of variance (ANOVA) (*, $P < 0.05$). Error bars, mean ± SE. OD, optical density.

distribution in plant (Wudick *et al.*, 2009). AtTIP4;1 was located in several endosomal membrane compartments and may localize on the plasma membrane (Liu *et al.*, 2003). AtTIP5;1 has been detected in pollen tube mitochondria membranes (Soto *et al.*, 2010) and McTIP1;2 was found in endosomes (Vera-Estrella *et al.*, 2004).

The subcellular targeting predictions by PSORT (Nakai & Horton, 1999) showed that PvTIP4;1 localized at the plasma membrane and some endosomal membrane compartments such as chloroplast thylakoid membrane, the Golgi body and endoplasmic reticulum membrane (Table S1). GFP fluorescence of PvTIP4;1 tagged constructs in *P. vittata* protoplasts was confined to a ring in the periphery of the protoplasts (Fig. 6f). The *PvTIP4;1–GFP* transgenic callus cells were stained with the plasma membrane marker FM4-64 and red fluorescence labeling was observed to overlapped with GFP (Fig. 7b). Both experiments indicated that PvTIP4;1 localized in the plasma of *P. vittata* cells. The localization of PvTIP4;1 results are similar to AtTIP4;1, which was hardly detected in the tonoplast. The difference is AtTIP4;1 was predicted to express in root endomembranes, but not exclude plasma membrane (Liu *et al.*, 2003). The tissue localization results showed a high and steady-state expression of *PvTIP4;1* in *P. vittata* sporophyte roots, while a relative low expression level in stipes and fronds (Fig. 8).

TIPs were reported to mediate the transport of water to regulate water flow in response to drought and salinity stress (Wudick *et al.*, 2009). In addition to their role as water channel proteins, TIPs also transport various solutes (glycerol, urea, hydrogen

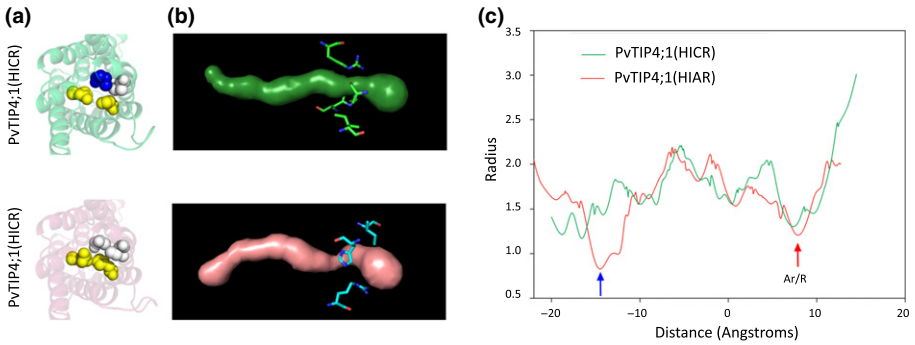

Fig. 11 Architecture of the aromatic/arginine (Ar/R) selectivity region and analyses of the putative pore radius of PvTIP4;1(HICR) and PvTIP4;1(HIAR). (a) Comparison of the Ar/R tetrad for PvTIP4;1(HICR) (green) and PvTIP4;1(HIAR) (red). The positions of the Ar/R residues from H2, H5, and loop E (LE1and LE2) are shown viewed perpendicular to the plane of the membrane. Residues are color coordinated according to charge and hydrophilicity: blue, basic hydrophilic; yellow, hydrophobic; white, neutral hydrophilic. (b) The pores of PvTIP4;1(HICR) (red) and PvTIP4;1(HIAR) (green) are viewed perpendicular to the pore axis and are labelled with respect to the location of the Ar/R regions. (c) Pore radius profiles of PvTIP4;1(HICR) (red) and PvTIP4;1(HIAR) (green). The red arrow indicates the approximate location of Ar/R constriction region. The blue arrow indicates the aperture which is more narrow than that of the Ar/R region of PvTIP4;1 (HICR). The position distance = 0 Å corresponds to the location of asparagine–proline–alanine (NPA) region. The radius of the pore regions of PvTIP4;1(HICR) and PvTIP4;1(HIAR) were analyzed and calculated by using the MOLE program and were visualized on PyMOL.

peroxide) (Wudick *et al.*, 2009), but the transport ability of As (III) was not reported previously. PvTIP4;1 is not induced by As (III) (Fig. 8), so PvTIP4;1 should also have its native functions in *P. vittata*.

Considering that PvTIP4;1 functions as a As(III) transporter in yeast and arsenic accumulator in *Arabidopsis*, expresses extremely highly on transcripts level in sporophytes root and localizes on the plasma membrane of *P. vittata* protoplasts the callus cells, we could speculate that *PvTIP4;1* may mediate As (III) uptake pathway.

So far, several genes involved in arsenic hyperaccumulation of *P. vittata* were identified and characterized, such as *PvACR2*, *PvGrx5* and *PvTP1*, which play an important role in As(V) reduction (Duan *et al.*, 2005; Ellis *et al.*, 2006; Rathinasabapathi *et al.*, 2006; Sundaram *et al.*, 2008); PvACR3, a protein that mediated As(III) efflux into the vacuole for sequestration (Indriolo *et al.*, 2010). Here, we found that *PvTIP4;1* may mediate As (III) uptake pathway in *P. vittata*, which might add a new gene member into *P. vittata*'s arsenic armory.

Moreover, sequence alignment showed that obvious differences between PvTIP4;1 and TIP4s from other plants reside within C-terminal cytoplasmic domains and LE1 position of Ar/R domain (Fig. 9; Table 1). Further investigates showed that expression of truncated $PvTIP4;1_{1\text{-}239}$ had no significant difference on metalloid sensitivity with *PvTIP4;1* (data not shown), while the substitution of cysteine in LE1 of PvTIP4;1 by alanine reduced the transport activities for As(III) (Fig. 10). It was reported that H2 position of AtNIP6;1 Ar/R filter is a critical determinant for transport substrate selectivity (Wallace & Roberts, 2005) and H5 position of Ar/R filter of both OsLsi1 and AtNIP5;1 plays a key role in the permeability to Si and B (Mitani-Ueno *et al.*, 2011). Our result showed the cysteine residue at the LE1 position in the ar/R domain of PvTIP4;1 is a functional site for arsenic transport and the transport activity was partially lost in the mutant of PvTIP4;1.

On the basis of report that the replacement of His with Val at H5 of AQP1 results in a wider Ar/R region that could accommodate the larger glycerol molecule (Wallace & Roberts, 2004), we constructed the homology model and analysis the pore diameter by the MOLE. The results showed that the diameter at the PvTIP4;1(HICR) Ar/R domain is larger than that of PvTIP4;1 (HIAR) (Fig. 11) and the larger diameter in the position of Ar/R tetrad may accommodate more solutes than PvTIP4;1(HIAR).

Most MIPs reported which confer arsenic transport in plant are from NIP and PIP families. Here, we identified a TIP subfamily aquaporin from *P. vittata*, PvTIP4;1, which may mediate As(III) uptake. Moreover, this work will provide a clue though the overall mechanism of arsenic hyperaccumulation of *P. vittata* is far from clear.

Acknowledgements

We thank Prof. Jingbo Jin and Ms Jingquan Li for providing technical advice. This study was supported by the National Natural Science Foundation of China (grants 31370299 and 31470549).

Author contributions

M.M., Y-G.Z., L.S. and Z.H. planned and designed the research. H.Y., Y.C., H.S., W.X., Z.H. and H.Z. performed experiments, conducted fieldwork, analyzed data, and so on. Z.H., H.Y. and Y.C. wrote the manuscript.

References

Adams A, Gottschling DE, Kaiser CA, Stearns T. 1997. *Methods in yeast genetics, 1997 edn.* New York, NY, USA: Cold Spring Harbor Laboratory Press, Cold Spring Harbor.

Agre P, Kozono D. 2003. Aquaporin water channels: molecular mechanisms for human diseases. *FEBS Letters* **555**: 72–78.

Barkla BJ, Vera-Estrella R, Pantoja O, Kirch HH, Bohnert HJ. 1999. Aquaporin localization – how valid are the TIP and PIP labels? *Trends in Plant Science* **4**: 86–88.

Bienert GP, Thorsen M, Schussler MD, Nilsson HR, Wagner A, Tamas MJ, Jahn TP. 2008. A subgroup of plant aquaporins facilitate the bi-directional diffusion of $As(OH)_{(3)}$ and $Sb(OH)_{(3)}$ across membranes. *BMC Biology* **6**: 15.

Bustin SA, Benes V, Garson JA, Hellemans J, Huggett J, Kubista M, Mueller R, Nolan T, Pfaffl MW, Shipley GL *et al.* 2009. The MIQE guidelines: minimum information for publication of quantitative real-time PCR experiments. *Clinical Chemistry* **55**: 611–622.

Cabello-Hurtado F, Ramos J. 2004. Isolation and functional analysis of the glycerol permease activity of two new nodulin-like intrinsic proteins from salt stressed roots of the halophyte *Atriplex nummularia*. *Plant Science* **166**: 633–640.

Chaumont F, Barrieu F, Wojcik E, Chrispeels MJ, Jung R. 2001. Aquaporins constitute a large and highly divergent protein family in maize. *Plant Physiology* **125**: 1206–1215.

Chen YS, Xu WZ, Shen HL, Yan HL, Xu WX, He ZY, Ma M. 2013. Engineering arsenic tolerance and hyperaccumulation in plants for phytoremediation by a *PvACR3* transgenic approach. *Environmental Science & Technology* **47**: 9355–9362.

Clough SJ, Bent AF. 1998. Floral dip: a simplified method for Agrobacterium-mediated transformation of *Arabidopsis thaliana*. *Plant Journal* **16**: 735–743.

Cullen WR, Reimer KJ. 1989. Arsenic speciation in the environment. *Chemical Reviews* **89**: 713–764.

Daniels MJ, Chaumont F, Mirkov TE, Chrispeels MJ. 1996. Characterization of a new vacuolar membrane aquaporin sensitive to mercury at a unique site. *Plant Cell* **8**: 587–599.

Danielson JAH, Johanson U. 2008. Unexpected complexity of the aquaporin gene family in the moss *Physcomitrella patens*. *BMC Plant Biology* **8**: 15.

DeLano WL, Lam JW. 2005. PyMOL: a communications tool for computational models. *Abstracts of Papers of the American Chemical Society* **230**: U1371–U1372.

Duan GL, Zhu YG, Tong YP, Cai C, Kneer R. 2005. Characterization of arsenate reductase in the extract of roots and fronds of Chinese brake fern, an arsenic hyperaccumulator. *Plant Physiology* **138**: 461–469.

Ellis DR, Gumaelius L, Indriolo E, Pickering IJ, Banks JA, Salt DE. 2006. A novel arsenate reductase from the arsenic hyperaccumulating fern *Pteris vittata*. *Plant Physiology* **141**: 1544–1554.

Fiser A, Sali A. 2003. MODELLER: generation and refinement of homology-based protein structure models. In: Carter CW, Sweet RM, eds. *Macromolecular crystallography, Part D*. San Diego, CA, USA: Elsevier Academic Press Inc, 461–491.

Fu DX, Libson A, Miercke LJW, Weitzman C, Nollert P, Krucinski J, Stroud RM. 2000. Structure of a glycerol-conducting channel and the basis for its selectivity. *Science* **290**: 481–486.

Gustavsson S, Lebrun AS, Norden K, Chaumont F, Johanson U. 2005. A novel plant major intrinsic protein in *Physcomitrella patens* most similar to bacterial glycerol channels. *Plant Physiology* **139**: 287–295.

Hayes RB. 1997. The carcinogenicity of metals in humans. *Cancer Causes and Control* **8**: 371–385.

Heymann JB, Engel A. 1999. Aquaporins: phylogeny, structure, and physiology of water channels. *News in Physiological Sciences* **14**: 187–193.

Hofte H, Hubbard L, Reizer J, Ludevid D, Herman EM, Chrispeels MJ. 1992. Vegetative and seed-specific forms of tonoplast intrinsic protein in the vacuolar membrane of *Arabidopsis thaliana*. *Plant Physiology* **99**: 561–570.

Indriolo E, Na G, Ellis D, Salt DE, Banks JA. 2010. A vacuolar arsenite transporter necessary for arsenic tolerance in the arsenic hyperaccumulating fern *Pteris vittata* is missing in flowering plants. *Plant Cell* **22**: 2045–2057.

Isayenkov SV, Maathuis FJM. 2008. The *Arabidopsis thaliana* aquaglyceroporin AtNIP7;1 is a pathway for arsenite uptake. *FEBS Letters* **582**: 1625–1628.

Jarup L. 2003. Hazards of heavy metal contamination. *British Medical Bulletin* **68**: 167–182.

Johanson U, Karlsson M, Johansson I, Gustavsson S, Sjovall S, Fraysse L, Weig AR, Kjellbom P. 2001. The complete set of genes encoding major intrinsic proteins in *Arabidopsis* provides a framework for a new nomenclature for major intrinsic proteins in plants. *Plant Physiology* **126**: 1358–1369.

Johnson KD, Herman EM, Chrispeels MJ. 1989. An abundant, highly conserved tonoplast protein in seeds. *Plant Physiology* **91**: 1006–1013.

Johnson KD, Hofte H, Chrispeels MJ. 1990. An intrinsic tonoplast protein of protein storage vacuoles in seeds is structurally related to a bacterial solute transporter (GlpF). *Plant Cell* **2**: 525–532.

Kamiya T, Tanaka M, Mitani N, Ma JF, Maeshima M, Fujiwara T. 2009. NIP1;1, an aquaporin homolog, determines the arsenite sensitivity of *Arabidopsis thaliana*. *Journal of Biological Chemistry* **284**: 2114–2120.

Kaur S, Kamli MR, Ali A. 2011. Role of arsenic and its resistance in nature. *Canadian Journal of Microbiology* **57**: 769–774.

Liu LH, Ludewig U, Gassert B, Frommer WB, von Wiren N. 2003. Urea transport by nitrogen-regulated tonoplast intrinsic proteins in Arabidopsis. *Plant Physiology* **133**: 1220–1228.

Liu ZJ, Shen J, Carbrey JM, Mukhopadhyay R, Agre P, Rosen BP. 2002. Arsenite transport by mammalian aquaglyceroporins AQP7 and AQP9. *Proceedings of the National Academy of Sciences, USA* **99**: 6053–6058.

Ma JF, Yamaji N, Mitani N, Xu XY, Su YH, McGrath SP, Zhao FJ. 2008. Transporters of arsenite in rice and their role in arsenic accumulation in rice grain. *Proceedings of the National Academy of Sciences, USA* **105**: 9931–9935.

Ma LQ, Komar KM, Tu C, Zhang WH, Cai Y, Kennelley ED. 2001. A fern that hyperaccumulates arsenic – a hardy, versatile, fast-growing plant helps to remove arsenic from contaminated soils. *Nature* **409**: 579.

Macur RE, Wheeler JT, McDermott TR, Inskeep WP. 2001. Microbial populations associated with the reduction and enhanced mobilization of arsenic in mine tailings. *Environmental Science & Technology* **35**: 3676–3682.

Meharg AA, Hartley-Whitaker J. 2002. Arsenic uptake and metabolism in arsenic resistant and nonresistant plant species. *New Phytologist* **154**: 29–43.

Meng YL, Liu ZJ, Rosen BP. 2004. As(III) and Sb(III) uptake by G1pF and efflux by ArsB in *Escherichia coli*. *Journal of Biological Chemistry* **279**: 18334–18341.

Mitani-Ueno N, Yamaji N, Zhao FJ, Ma JF. 2011. The aromatic/arginine selectivity filter of NIP aquaporins plays a critical role in substrate selectivity for silicon, boron, and arsenic. *Journal of Experimental Botany* **62**: 4391–4398.

Mosa KA, Kumar K, Chhikara S, McDermott J, Liu ZJ, Musante C, White JC, Dhankher OP. 2012. Members of rice plasma membrane intrinsic proteins subfamily are involved in arsenite permeability and tolerance in plants. *Transgenic Research* **21**: 1265–1277.

Mudhoo A, Sharma SK, Garg VK, Tseng CH. 2011. Arsenic: an overview of applications, health, and environmental concerns and removal processes. *Critical Reviews in Environmental Science and Technology* **41**: 435–519.

Nakai K, Horton P. 1999. PSORT: a program for detecting sorting signals in proteins and predicting their subcellular localization. *Trends in Biochemical Sciences* **24**: 34–35.

Quigley F, Rosenberg JM, Shachar-Hill Y, Bohnert HJ. 2002. From genome to function: the *Arabidopsis* aquaporins. *Genome Biology* **3**: 17.

Rathinasabapathi B, Wu S, Sundaram S, Rivoal J, Srivastava M, Ma LQ. 2006. Arsenic resistance in *Pteris vittata* L.: identification of a cytosolic triosephosphate isomerase based on cDNA expression cloning in *Escherichia coli*. *Plant Molecular Biology* **62**: 845–857.

Sehnal D, Varekovaa RS, Berka K, Pravda L, Navratilova V, Banas P, Ionescu CM, Otyepka M, Koca J. 2013. MOLE 2.0: advanced approach for analysis of biomacromolecular channels. *Journal of Cheminformatics* **5**: 13.

Soto G, Fox R, Ayub N, Alleva K, Guaimas F, Erijman EJ, Mazzella A, Amodeo G, Muschietti J. 2010. TIP5;1 is an aquaporin specifically targeted to pollen mitochondria and is probably involved in nitrogen remobilization in *Arabidopsis thaliana*. *Plant Journal* **64**: 1038–1047.

Spyropoulos IC, Liakopoulos TD, Bagos PG, Hamodrakas SJ. 2004. TMRPres2D: high quality visual representation of transmembrane protein models. *Bioinformatics* **20**: 3258–3260.

Stroud RM, Savage D, Miercke LJW, Lee JK, Khademi S, Harries W. 2003. Selectivity and conductance among the glycerol and water conducting aquaporin family of channels. *FEBS Letters* **555**: 79–84.

Sui HX, Han BG, Lee JK, Walian P, Jap BK. 2001. Structural basis of water-specific transport through the AQP1 water channel. *Nature* **414**: 872–878.

Sundaram S, Rathinasabapathi B, Ma LQ, Rosen BP. 2008. An arsenate-activated glutaredoxin from the arsenic hyperaccumulator fern *Pteris vittata*

L. regulates intracellular arsenite. *Journal of Biological Chemistry* **283**: 6095–6101.

Tamura K, Peterson D, Peterson N, Stecher G, Nei M, Kumar S. 2011. MEGA5: molecular evolutionary genetics analysis using maximum likelihood, evolutionary distance, and maximum parsimony methods. *Molecular Biology and Evolution* **28**: 2731–2739.

Vera-Estrella R, Barkla BJ, Bohnert HJ, Pantoja O. 2004. Novel regulation of aquaporins during osmotic stress. *Plant Physiology* **135**: 2318–2329.

Wallace IS, Roberts DM. 2004. Homology modeling of representative subfamilies of Arabidopsis major intrinsic proteins. Classification based on the aromatic/arginine selectivity filter. *Plant Physiology* **135**: 1059–1068.

Wallace IS, Roberts DM. 2005. Distinct transport selectivity of two structural subclasses of the nodulin-like intrinsic protein family of plant aquaglyceroporin channels. *Biochemistry* **44**: 16826–16834.

Wang X, Ma LQ, Rathinasabapathi B, Cai Y, Liu YG, Zeng GM. 2011. Mechanisms of efficient arsenite uptake by arsenic hyperaccumulator *Pteris vittata*. *Environmental Science & Technology* **45**: 9719–9725.

Weig A, Deswarte C, Chrispeels MJ. 1997. The major intrinsic protein family of Arabidopsis has 23 members that form three distinct groups with functional aquaporins in each group. *Plant Physiology* **114**: 1347–1357.

Wistow GJ, Pisano MM, Chepelinsky AB. 1991. Tandem sequence repeats in transmembrane channel proteins. *Trends in Biochemical Sciences* **16**: 170–171.

Wudick MM, Luu DT, Maurel C. 2009. A look inside: localization patterns and functions of intracellular plant aquaporins. *New Phytologist* **184**: 289–302.

Wysocki R, Chery CC, Wawrzycka D, Van Hulle M, Cornelis R, Thevelein JM, Tamas MJ. 2001. The glycerol channel Fps1p mediates the uptake of arsenite and antimonite in *Saccharomyces cerevisiae*. *Molecular Microbiology* **40**: 1391–1401.

Xu W, Dai W, Yan H, Li S, Shen H, Chen Y, Xu H, Sun Y, He Z, Ma M. 2015. *Arabidopsis* NIP3;1 plays an important role in arsenic uptake and root-to-shoot translocation under arsenite stress conditions. *Molecular Plant* **8**: 722–733.

Xu XY, McGrath SP, Zhao FJ. 2007. Rapid reduction of arsenate in the medium mediated by plant roots. *New Phytologist* **176**: 590–599.

Yang M. 2011. A current global view of environmental and occupational cancers. *Journal of Environmental Science and Health Part C-Environmental Carcinogenesis & Ecotoxicology Reviews* **29**: 223–249.

Yang X, Chen H, Xu W, He Z, Ma M. 2007. Hyperaccumulation of arsenic by callus, sporophytes and gametophytes of *Pteris vittata* cultured *in vitro*. *Plant Cell Report* **26**: 1889–1897.

Yamamura S, Watanabe M, Kanzaki M, Soda S, Ike M. 2008. Removal of arsenic from contaminated soils by microbial reduction of arsenate and quinone. *Environmental Science & Technology* **42**: 6154–6159.

Yoo SD, Cho YH, Sheen J. 2007. Arabidopsis mesophyll protoplasts: a versatile cell system for transient gene expression analysis. *Nature Protocols* **2**: 1565–1572.

Supporting Information

Additional supporting information may be found in the online version of this article.

Fig. S1 Seed germination rate of transgenic *Arabidopsis* plants expressing *PvTIP4;1*.

Fig. S2 Topology of GlpF PvTIP4;1(HICR) and PvTIP4;1 (HIAR) and architecture of the Ar/R selectivity region.

Table S1 Proteins and GenBank ID numbers for the phylogenetic analysis

Table S2 The data produced according to the MIQE guidelines for tissues expression of *PvTIP4;1* in *P. vittata* sporophyte

Table S3 Final result information of the PSORT software on prediction of PvTIP4;1 localization

Please note: Wiley Blackwell are not responsible for the content or functionality of any supporting information supplied by the authors. Any queries (other than missing material) should be directed to the *New Phytologist* Central Office.